

# HIF-1 is involved in high glucose-induced paracellular permeability of brain endothelial cells

Jingqi Yan · Ziyang Zhang · Honglian Shi

Received: 18 January 2011 / Revised: 22 April 2011 / Accepted: 9 May 2011 / Published online: 27 May 2011  
© Springer Basel AG 2011

**Abstract** Experimental evidence from human patients and animal models of diabetes has demonstrated that hyperglycemia increases blood–brain barrier (BBB) permeability, which is associated with increased risk of neurological dysfunction. However, the mechanism underlying high glucose-induced BBB disruption is not understood. Here we investigated the role of hypoxia-inducible factor-1 (HIF-1) in high glucose-induced endothelial permeability in vitro using mouse brain microvascular endothelial cells (b.End3). Our results demonstrated that high glucose (30 mM) upregulated the protein level of HIF-1 $\alpha$ , the regulatable subunit of HIF-1, and increased the transcriptional activity of HIF-1 in the endothelial cells. At the same time, high glucose increased the paracellular permeability associated with diminished expression and disrupted continuity of tight junction proteins occludin and zona occludens protein-1 (ZO-1) of the endothelial cells. Upregulating HIF-1 activity by cobalt chloride increased the paracellular permeability of the endothelial cells exposed to normal glucose (5.5 mM). In contrast, downregulating HIF-1 activity by HIF-1 $\alpha$  inhibitors and HIF-1 $\alpha$  specific siRNA ameliorated the increased paracellular permeability and the alterations of distribution pattern of occludin and ZO-1 induced by high glucose. In addition, high glucose increased expression of vascular endothelial growth factor (VEGF), a downstream gene of HIF-1. Inhibiting VEGF improved the expression pattern of occludin and ZO-1, and attenuated the endothelial leakage. Furthermore, key results were confirmed in human brain

microvascular endothelial cells. These results strongly indicate that HIF-1 plays an important role in high glucose-induced BBB dysfunction. The results will help us understand the molecular mechanisms involved in hyperglycemia-induced BBB dysfunction and neurological outcomes.

**Keywords** Diabetes · High glucose · Blood–brain barrier · Permeability · HIF-1 · VEGF

## Abbreviations

BBB	Blood–brain barrier
HIF-1	Hypoxia-inducible factor 1
VEGF	Vascular endothelial growth factor
2ME2	2-Methoxyestradiol
YC-1	3-(5'-Hydroxymethyl-2'-furyl)-1-benzyl indazole
ZO-1	Zona occludens protein-1

## Introduction

Neurological complications are among the central problems in diabetes mellitus. Over 60% of individuals with diabetes are affected by neurological disorders [1, 2]. Vascular dysfunction plays a major role in many complications associated with diabetes as evident in clinical studies such as the Diabetes Control and Complications Trial in patients with type I diabetes [3] and the UK Prospective Diabetes Study in patients with type II diabetes [4]. While studies on cerebral microvasculature under exposure to hyperglycemia are lagging behind those on peripheral vessels [5], accumulating evidence indicates that diabetes is associated with considerable alterations in the permeability of blood–brain barrier (BBB). For example, in 1980s it was reported that the BBB of diabetic animals

J. Yan · Z. Zhang · H. Shi (✉)  
Department of Pharmacology and Toxicology,  
School of Pharmacy, University of Kansas,  
1251 Wescoe Hall Drive, Malott Hall 5044, Lawrence,  
KS 66045, USA  
e-mail: hshi@ku.edu

manifested an increased permeability shortly (< 4 weeks) after diabetic induction [6, 7]. Since then, compromised BBB has been documented in animal models of diabetes by many groups [8–11]. Furthermore, BBB dysfunction has been confirmed in human diabetic patients [12, 13] as brain imaging technology advances. However, the mechanism of diabetes-induced BBB dysfunction is not clear.

BBB forms a neurovascular unit that protects the brain from circulating neurotoxic agents and inflammatory factors while maintaining nutrients and ions in the brain at levels suitable for brain function. The integrity of endothelial cell-cell junctions and the BBB function are regulated by a series of adhesion molecules that make up tight junctions (TJ). Among these molecules, occludin and claudins are the major TJ component proteins. Zona occludens protein-1 (ZO-1), also known as TJ protein 1, binds both occludin and claudin directly. In addition, ZO-1 engages in intracellular interactions with signaling molecules and transcription factors [14]. Studies have shown that alteration of the expression and arrangement of these proteins causes endothelial leakage at BBB [15, 16]. BBB dysfunction compromises synaptic and neuronal functions and contributes to the progression of neurological diseases [17]. Understanding the mechanism of BBB integrity disruption may provide a novel therapeutic target in diabetes-associated neurological complications.

Hypoxia inducible factor 1 (HIF-1) is a transcriptional factor that activates genes involved in cellular adaptation to hypoxia by facilitating oxygen supply, glucose transport, new blood vessel formation, etc. Among the genes regulated by HIF-1, vascular endothelial growth factor (VEGF) is well defined in promoting new blood vessel formation, altering the structure of vasculature and causing vascular remodeling [18]. It is known that VEGF causes BBB disruption and increases BBB permeability [19, 20], possibly by altering TJ proteins such as ZO-1 [9, 15, 21] and occludin [9, 21]. High glucose has been reported to upregulate HIF-1 activity in isolated hearts of rats [22], mouse kidney mesangial cells [23], human mesangial cells [23], etc. However, it is not known if HIF-1 is induced in and involved in permeability dysfunction of brain endothelial cells exposed to high glucose.

The purpose of the present study was to determine whether or not high glucose induced HIF-1 activity in brain endothelial cells and, if so, whether or not HIF-1 played a role in high glucose-induced BBB permeability. The study was carried out with an *in vitro* BBB model of mouse brain microvascular endothelial cells (b.End3). Previous publications have well characterized b.End3 as an appropriate model of *in vitro* BBB [24–26], which has been widely used to study mechanisms of BBB disruption in various pathological conditions [20, 27–30]. In addition, primary human brain microvascular endothelial cells (hBMVECs) [30, 31] were used to confirm major findings from the

mouse cells. The study provided direct evidence that HIF-1 played an important role in high glucose-induced increase in brain endothelial permeability.

## Materials and methods

### Cell culture and treatments

Mouse cerebral microvascular endothelial cells (b.End3) (ATCC, Manassas, VA) were cultured in Dulbecco's Modified Eagle's Medium (DMEM, 5.5 mM glucose) with 10% fetal bovine serum (Hyclone, Logan, UT) plus penicillin/streptomycin (Invitrogen, Carlsbad, CA). Primary human brain microvascular endothelial cells (hBMVECs) were obtained from ScienCell Research Laboratories (Carlsbad, CA) and were used at passage 1 or 2. After growing the cells to confluency, the cell cultures were maintained in DMEM with various glucose concentrations (5.5, 30 or 50 mM) for 1, 3, 6 or 10 days. In the text, "glucose" refers to D-glucose unless otherwise noted. To determine whether the effect of high glucose (30 and 50 mM) resulted from osmotic changes of culture medium, effects of L-glucose at 30 and 50 mM were tested [32].

Two HIF-1 inhibitors were used to examine the effect of HIF-1 on high glucose-induced endothelial permeability, 3-(5'-hydroxymethyl-2'-furyl)-1-benzyl indazole (YC-1) (Cayman, Ann Arbor, MI) and 2-methoxyestradiol (2ME2) (ENZO, Plymouth Meeting, PA) [20, 33, 34]. For inhibitor experiments, 10  $\mu$ M YC-1 or 10  $\mu$ M 2ME2 was added to cell cultures 2 h before the addition of high glucose and added with each medium change, which was conducted every 2 days. Besides YC-1 and 2ME2, we also used HIF-1 $\alpha$ -specific siRNA to inhibit HIF-1 $\alpha$  expression in b.End3 cells. The predesigned siRNA for mouse HIF-1 $\alpha$  (SI00193011) and the negative control siRNA (1027280) were purchased from Qiagen (Valencia, CA). The HIF-1 $\alpha$  siRNA was transfected into b.End3 cells plated in 6-well plates with the transfection reagent Hiperfect (Qiagen) before the addition of high glucose. For the 6-day treatment, siRNA transfections were conducted every 2 days according to the manufacturer's procedure. To inhibit the activity of VEGF, VEGF antibody (Ab-VEGF, sc-507, Santa Cruz, Santa Cruz, CA) at 100 ng/ml (final concentration) was added to the cell culture medium 2 h before the high glucose (30 mM) treatment based on a previous report [21]. The cell culture medium was changed every 2 days with addition of the VEGF antibody to the new culture medium.

### Paracellular permeability assay

The paracellular permeability was detected as described previously [20]. Briefly, cells were plated on the cell

culture inserts (diameter, 10 mm; pore size, 0.4  $\mu\text{m}$ ; polycarbonate membrane, Nalge Nunc International, Rochester, NY). After reaching confluency, cells were treated with high glucose for 1, 3, 6 or 10 days. Fluorescein isothiocyanate (FITC)-dextran (1 mg/ml, 500  $\mu\text{l}$ ; Sigma, St. Louis, MO) was added to the cell culture medium inside the inserts 3 h before the end of the indicated time periods. FITC-dextran with two different molecular sizes (40 and 70 kDa) was tested. After incubation for 3 h, 50  $\mu\text{l}$  of medium from the outside of the insert was taken out and diluted to 500  $\mu\text{l}$  with PBS. Fluorescence intensity of FITC-dextran was measured at the excitation wavelength of 492 nm and the emission wavelength of 520 nm by a fluorescent multi-mode microplate reader (Biotek, Winooski, VT). To avoid a time-based FITC increase in the lower chamber, the time-based study was not carried out with the same inserts, but with different groups of inserts. The permeability coefficient was calculated based on previous reports [24, 35].

#### Plasmid transfection and luciferase activity assay

The plasmid PGL2TkHRE containing the hypoxia response element (HRE) and the firefly luciferase gene was a gift from Dr. Giovanni Melillo at the National Cancer Institute in Frederick, MD [36]. After a 6-day treatment of high glucose with or without HIF-1 $\alpha$  inhibition, cells grown in 24-well plates were transfected with PGL2TkHRE by using the transfection reagent Lipofectamine 2000 (Invitrogen, Carlsbad, CA). As a positive control, cobalt chloride at 100  $\mu\text{M}$  was added to cells 24 h after transfection [37]. Forty-eight hours after the transfection, luciferase activity was measured with the Luciferase Assay System (Promega, Madison, WI) on a micro-plate Luminometer (Berthold, Oak Ridge, TN).

#### Western blot assay

Cells were lysed in RIPA (RadioImmunoPrecipitation Assay) buffer with a cocktail of protease inhibitors (Thermo, Meridian, IL). The protein concentration was determined by the Bio-Rad DC protein assay reagent (Bio-Rad, Hercules, CA). Standard Western blot procedures were conducted with primary antibodies HIF-1 $\alpha$  (610959, BD Biosciences, San Jose, CA), ZO-1 (40-2200, Invitrogen, Carlsbad, CA), occludin (33-1500, Invitrogen), claudin-5 (34-1600, Invitrogen), VEGF (sc-507, Santa Cruz) and  $\beta$ -actin (sc-1616, Santa Cruz). The signal development was carried out with an enhanced chemiluminescence detection kit (Pierce, Rockford, IL). The intensity of immunoreactive bands was quantified using Image-J. Results were normalized to  $\beta$ -actin.

#### Immunocytochemistry

After being exposed to high glucose for 6 days with or without HIF-1 $\alpha$  inhibitors, cells grown on L-lysine coated coverslips were washed three times with PBS and fixed with 4% paraformaldehyde in PBS at room temperature for 20 min. After being blocked with PBS containing 0.05% triton-X100 and 0.25% BSA for 45 min, cells were incubated with the primary antibodies against ZO-1, occludin or claudin-5 (Invitrogen) in the blocking solution at 4°C overnight. After three washes, cells were incubated with a fluorescent secondary antibody (goat anti-rabbit Alexa 488 for ZO-1 and claudin-5, and donkey anti-mouse Alexa 488 for occludin, Molecular Probes, Carlsbad, CA). After washing, the coverslips were mounted with Vectashield (Vector Laboratories, Burlingame, CA). Images were captured under a Leica DMI 4000B fluorescent microscope (Leica, Bannockburn, IL).

#### Statistical analysis

One-way ANOVA was used to determine overall significance of difference in various assays followed by post hoc Tukey's tests corrected for multiple comparisons. Data were presented as means  $\pm$  SEM. Differences were considered statistically significant at  $p < 0.05$ .

## Results

### High glucose increased HIF-1 activity in b.End3 endothelial cells

HIF-1 is a heterodimer that is composed of  $\alpha$  and  $\beta$  subunits. It is known that HIF-1 $\alpha$  protein is continuously synthesized, but rapidly degraded in normoxic cells. HIF-1 $\beta$  is constitutively expressed in cells and relatively stable. The HIF-1 $\alpha$  protein level primarily determines HIF-1 activity [38, 39]. Therefore, we focused on the protein expression of HIF-1 $\alpha$  in b.End3 cells after exposure to high glucose. In this study, 30 and 50 mM were used as high glucose with 5.5 mM as normal control. The rationale of exposing cells to 30 and 50 mM glucose to mimic hyperglycemia has been well documented in a previous publication [32]. Figure 1 shows that high glucose induced HIF-1 $\alpha$  expression time-dependently. In the first 24 h of exposure, HIF-1 $\alpha$  expression was increased slightly but not significantly. A significant increase in HIF-1 $\alpha$  expression was observed in the cells exposed to high glucose for 3, 6 and 10 days. Furthermore, at each of those time points, 50 mM glucose induced more HIF-1 $\alpha$  expression than 30 mM. To determine if the increase in HIF-1 $\alpha$  expression was due to osmotic changes, cells were treated with

L-glucose at 50 mM in the presence of 5.5 mM D-glucose. Although the HIF-1 $\alpha$  level in L-glucose-treated cells seemed to increase with the exposure periods, there was no significant difference compared to the controls (5.5 mM D-glucose) at the same time points.

As a transcriptional factor, the most important indicator of HIF-1 function is its transcriptional activity. To confirm that high glucose did increase HIF-1 function, we measured its transcriptional activity in b.End3 cells after exposure to high glucose. To study the transcriptional activity, b.End3 cells were transfected with the plasmid PGL2TkHRE containing the HRE-luciferase reporter gene. As shown in Table 1, exposure to glucose at 30 and 50 mM for 6 days elevated the luciferase activity by 65 and 83%, respectively, while 50 mM L-glucose in the presence of 5.5 mM D-glucose had no significant effect. These results indicate that high glucose increased not only the protein level of HIF-1 $\alpha$ , but also the transcriptional activity of HIF-1 in the brain endothelial cells.

#### High glucose increased paracellular permeability of b.End3 endothelial cells

Next, we examined how high glucose affected the paracellular permeability of b.End3 cells. We first tested the permeability to dextran 40 kDa based on a previous publication [20]. The basal level of the permeability was  $3.24 \pm 0.43 \times 10^{-6}$  cm/s. Similar to its effect on HIF-1 $\alpha$  protein expression, high glucose caused a time-dependent increase in endothelial paracellular permeability (Fig. 2).

**Fig. 1** Time-dependent effects of high glucose on HIF-1 $\alpha$  expression in b.End3 cells. Cells were treated with glucose (D-glucose unless otherwise noted) at 5.5, 30 and 50 mM for 1, 3, 6 or 10 days. L-Glucose at 50 mM in the presence of 5.5 mM D-glucose was used as osmotic control (50 L). **a** Representative Western blots of HIF-1 $\alpha$  with  $\beta$ -actin as a protein loading control. **b** Summary of three independent experiments. Values were normalized to  $\beta$ -actin and control (5.5 mM glucose, 1 day). Data are means  $\pm$  SEM,  $n = 3$ . \* $p < 0.05$  versus 3 day control (5.5 mM glucose), # $p < 0.05$  versus 6 day control (5.5 mM glucose), @ $p < 0.05$  versus 10 day control (5.5 mM glucose)

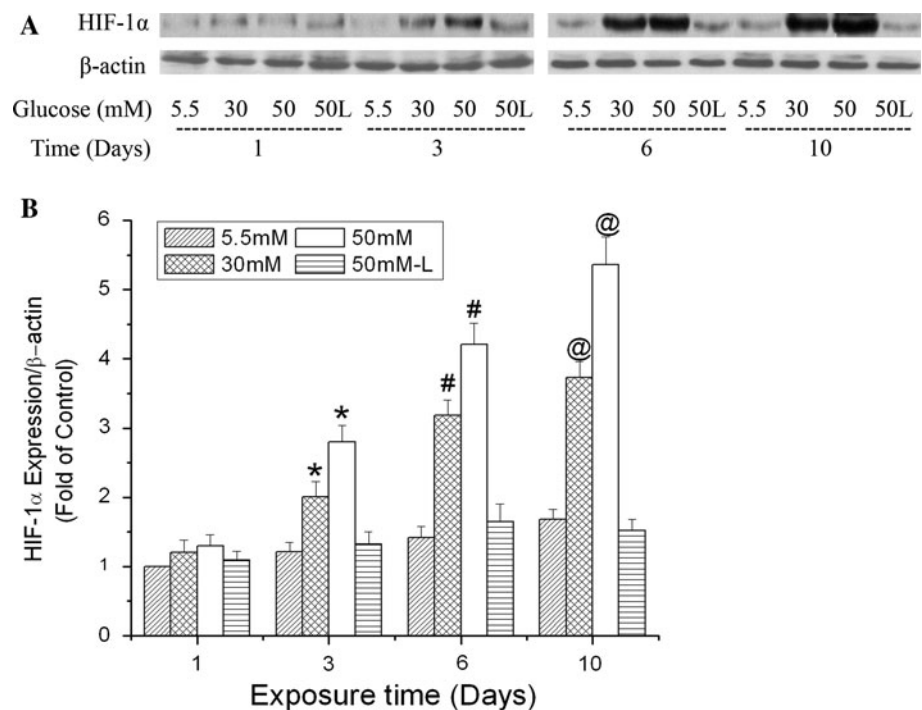


**Table 1** Effects of high glucose on the transcriptional activity of HIF-1

	A.U./ $\mu$ g ml $^{-1}$	% change
Control (5.5 mM)	46.4 $\pm$ 7.0	–
High glucose (30 mM)	76.5 $\pm$ 6.2*	65
High glucose (50 mM)	84.9 $\pm$ 8.3*	83
L-glucose (50 mM)	48.7 $\pm$ 7.5	5

B.End3 cells were treated with various glucose concentrations for 6 days. Values were normalized to control (5.5 mM glucose). Data are means  $\pm$  SEM,  $n = 3$

A.U. arbitrary unit

\*  $p < 0.05$  versus control

After 1-day exposure, there was no difference in permeability between control and cells exposed to high glucose. After 3 days, glucose at both 30 and 50 mM increased the permeability. The increase in permeability became more significant as the exposure time was prolonged to 6 or 10 days. The permeability on day 10 was  $14.76 \pm 0.91$  and  $18.56 \pm 1.16 \times 10^{-6}$  cm/s for 30 and 50 mM glucose-treated cells, respectively. The figure also demonstrates that higher glucose concentration (50 mM) led to a greater increase in paracellular permeability than the lower glucose (30 mM) after 3, 6 or 10 day treatments. In addition, L-glucose at 30 or 50 mM had no effect on the paracellular permeability at all the time points.

Furthermore, we tested the effect of high glucose on the paracellular permeability to a higher molecular size



(dextran 70 kDa). As shown in Fig. 2b, the permeability coefficient to dextran 70 kDa was much smaller than that to dextran 40 kDa. The basal level of the permeability to dextran 70 kDa was  $0.74 \pm 0.05 \times 10^{-6}$  cm/s, indicating less passage of higher molecular weights. Glucose at 50 mM but not 30 mM increased the permeability to 70 kDa dextran in 3 days. After 6 days, glucose at 30 mM started to significantly increase the permeability to dextran 70 kDa. The result indicates that the high glucose-mediated alteration of the permeability coefficient to dextran 70 kDa was slower than to dextran 40 kDa. L-Glucose did not have any effect on the permeability to dextran 70 kDa.

Given the important role of ZO-1, occludin and claudin-5 in TJ assembly and maintenance of the barrier function [15, 16], their protein expression level and arrangement pattern were studied by Western blotting and

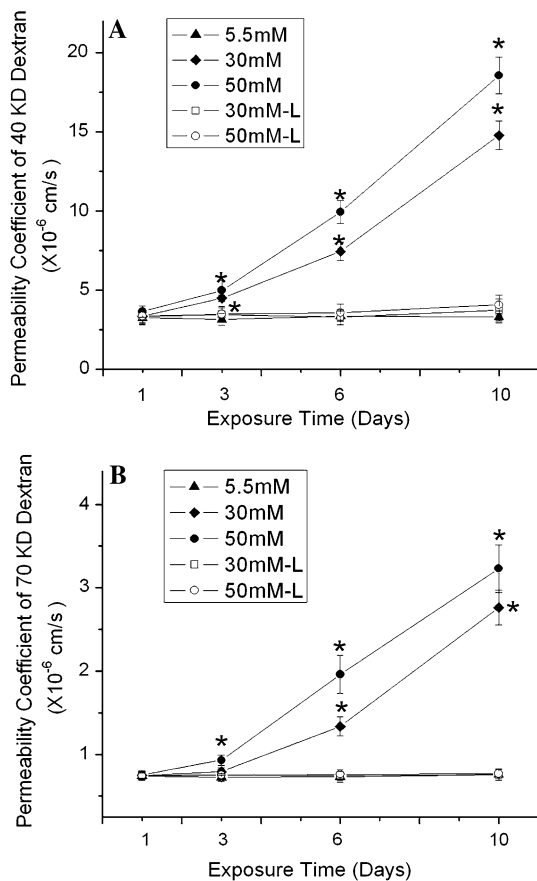


**Fig. 2** Effects of high glucose on paracellular permeability of b.End3 cells. The permeability was determined with 40 kDa (a) and 70 kDa (b) FITC-dextran. Cells were treated with glucose at 5.5, 30 and 50 mM for 1, 3, 6 or 10 days. L-Glucose at both 30 and 50 mM in the presence of 5.5 mM D-glucose was used as osmotic control. Permeability was described as absolute values of coefficients. Values are means  $\pm$  SEM,  $n = 3$ . \* $p < 0.05$  versus control (1 day, 5.5 mM glucose)

immunocytochemical labeling to further characterize high glucose-induced paracellular permeability. Fig. 3a demonstrates that high glucose decreased the protein expression level of ZO-1 and occludin in b.End3 cells on day 3 and thereafter. The degree of decrease of ZO-1 was more severe than that of occludin on day 3. The ZO-1 level was reduced 68 and 62% by 30 and 50 mM glucose, respectively, in 3 days, and remained at this low level as the exposure time was prolonged to 6 or 10 days (Fig. 3b). The occludin level decreased 32 and 36% by 30 and 50 mM glucose, respectively, in 3 days. It decreased further as the exposure time was prolonged to 6 or 10 days (Fig. 3c). The protein expression of claudin-5, however, was relatively stable in the cells exposed to high glucose (Fig. 3d). During the 10-day exposure, L-glucose at 50 mM in the presence of 5.5 mM D-glucose did not induce significant changes of ZO-1, occludin and claudin-5 expression compared with control (5.5 mM glucose) at the same time points. Furthermore, results from immunocytochemical staining confirmed that high glucose altered the arrangement pattern of ZO-1 and occludin, but not claudin-5 after exposure for 6 days (Fig. 3e). In other words, high glucose disrupted the continuity of the ZO-1 and occludin staining. These results support the observed permeability increase of the endothelial monolayer by high glucose and suggest that disruption of ZO-1 and occludin may be the potential reason for increased permeability.

#### Upregulating HIF-1 activity increased paracellular permeability of b.End3 cells

The above experiments indicate a positive correlation between HIF-1 expression and permeability increase of b.End3 cells exposed to high glucose. To determine the role of HIF-1 in high glucose-induced paracellular permeability increase, we carried out experiments with upregulation of HIF-1 $\alpha$  in cells exposed to normal glucose (5.5 mM). If HIF-1 played a role in the high-glucose-induced permeability, upregulation of HIF-1 expression would increase the paracellular permeability of endothelial cells cultured in normal glucose. It is well established that cobalt chloride can inhibit HIF-1 $\alpha$  degradation and increase HIF-1 activity. To test the concept, the endothelial monolayer was exposed to 100  $\mu$ M cobalt chloride. Co<sup>++</sup> was able to increase the HIF-1 $\alpha$  protein level and HIF-1 transcriptional activity in b.End3 cells exposed to 5.5 mM glucose (Fig. 5a-c). At the same time, Co<sup>++</sup> induced a time-dependent increase in the paracellular permeability (Fig. 4). Furthermore, images of immunostained cells demonstrate that Co<sup>++</sup> treatments reduced the expression level of ZO-1 and occludin, and disorganized their arrangements (Fig. 5d). This result is in agreement with a

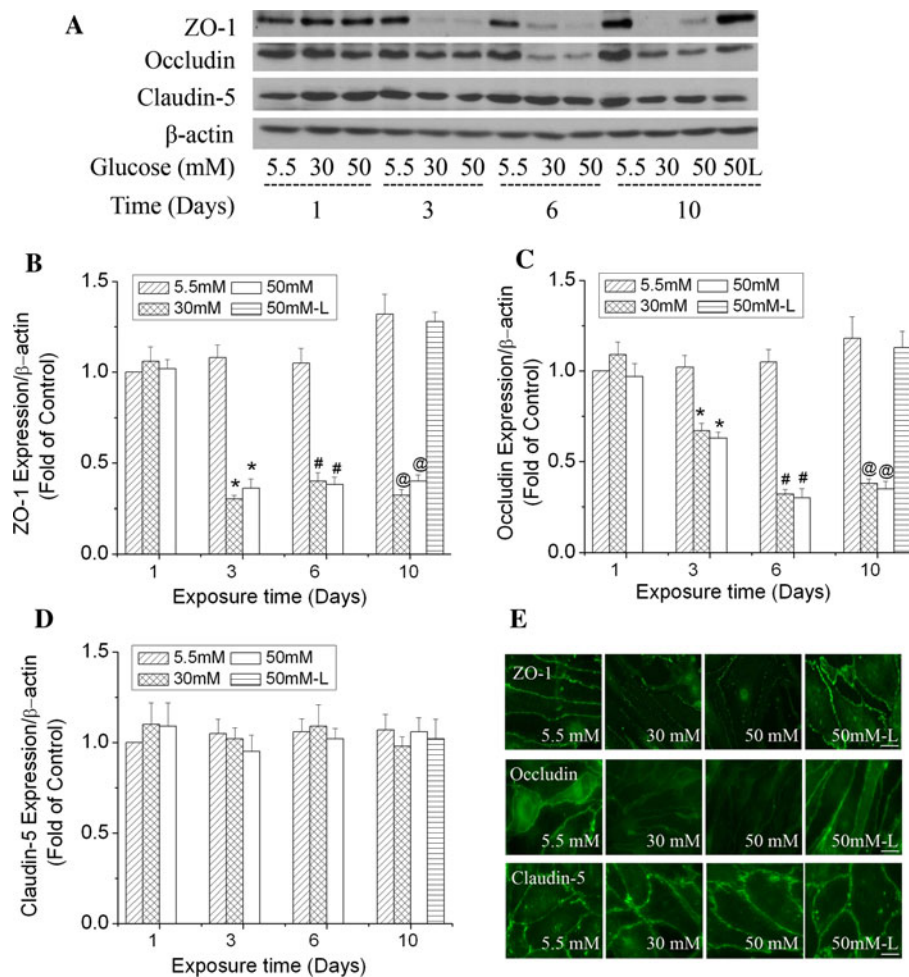


**Fig. 3** Time-dependent effects of high glucose on the expression and arrangement of ZO-1, occludin and claudin-5 in b.End3 cells. Cells were treated with glucose at 5.5, 30 and 50 mM for 1, 3, 6 or 10 days. L-Glucose at 50 mM in the presence of 5.5 mM D-glucose was used as osmotic control (50 L). **a** Representative Western blots of ZO-1, occludin and claudin-5 after high glucose treatments.  $\beta$ -actin served as a protein loading control. **b** Summary of the protein level of ZO-1. **c** Summary of the protein level of occludin. **d** Summary of the protein

level of claudin-5. **e** Representative images of ZO-1, occludin and claudin-5 immunostaining after cells were exposed to 30 mM glucose for 6 days. Scale bar 22  $\mu$ m. L-Glucose at 50 mM in the presence of 5.5 mM D-Glucose was used as osmotic control. Values in **b**, **c** and **d** were normalized to  $\beta$ -actin and control (5.5 mM glucose). Values are means  $\pm$  SEM,  $n = 3$ . \* $p < 0.05$  versus 3 day control (5.5 mM glucose), # $p < 0.05$  versus 6 day control (5.5 mM glucose), @ $p < 0.05$  versus 10 day control (5.5 mM glucose)

previous report that  $\text{Co}^{++}$  could induce paracellular permeability [20].

Inhibiting HIF-1 $\alpha$  expression attenuated paracellular permeability of b.End3 cells

To further verify the role of HIF-1 in high glucose-induced paracellular permeability increase, we carried out experiments with inhibition of HIF-1 by HIF-1 $\alpha$  inhibitors and HIF-1 $\alpha$ -specific siRNA. As seen in Fig. 5a–c, specific inhibition of HIF-1 $\alpha$  expression by siRNA (10 nM) transfection significantly reduced the protein expression level of HIF-1 $\alpha$  and the transcription activity of HIF-1 in b.End3 cells exposed to 30 mM glucose for 6 days. HIF-1 $\alpha$  siRNA-transfected cells showed enhanced expression and

arrangement patterns of ZO-1 and occludin (Fig. 5d). The siRNA inhibition remarkably decreased the increase in paracellular permeability caused by high glucose (Fig. 5e). In addition, the effects of two widely used HIF-1 inhibitors, YC-1 and 2ME2, were tested. Both 2ME2 and YC-1 at 10  $\mu$ M effectively decreased HIF-1 expression and its transcriptional activity (Fig. 5a–c), and reduced the permeability increase caused by high glucose (Fig. 5f). It is worth noting that HIF-1 activity of the cells treated with YC-1, 2ME2 and HIF-1 $\alpha$  siRNA was lower than that of controls (Fig. 5c). This indicates that there is a basal level of HIF-1 activity in control cells as previously reported [40, 41] and that the HIF-1 inhibitors suppressed the basal activity. All these results are evidence that downregulating HIF-1 activity reduced alterations of ZO-1 and occludin

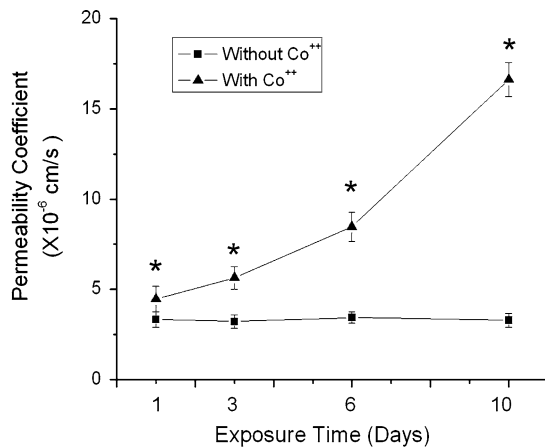


**Fig. 4** Effects of cobalt chloride on the paracellular permeability of b.End3 cells. The permeability was measured using 40 kDa FITC-dextran. Cells were cultured under normal condition (5.5 mM glucose) in the presence of 100  $\mu$ m cobalt chloride for 1, 3, 6 or 10 days. Permeability was described as absolute values of coefficients. Values are means  $\pm$  SEM,  $n = 3$ . \* $p < 0.05$  versus control

expression, and attenuated the increased paracellular permeability, confirming a robust role of HIF-1 in high glucose-induced permeability increase.

#### VEGF contributes to HIF-1's effect on permeability

VEGF is an essential downstream effector of HIF-1 and has been reported to be involved in BBB disruption. We explored its role in high glucose-induced permeability. Coinciding with changes of HIF-1 $\alpha$  expression, changes in the level of VEGF protein expression were time-dependent (Fig. 6). In the first 24 h of exposure, high glucose did not increase VEGF expression. Increases in VEGF expression were observed in the cells exposed to both 30 and 50 mM glucose for 3, 6 and 10 days. At each time point, 50 mM glucose induced more VEGF expression than 30 mM; 50 mM L-glucose in the presence of 5.5 mM D-glucose had no significant effect on the protein content of VEGF at any of the time points tested.

To verify the role of VEGF in high glucose-induced paracellular permeability increase, the VEGF level was also detected after HIF-1 activation or inhibition (Fig. 7a, b). HIF-1 activator, cobalt chloride, increased the VEGF level by 39%. At the same time, HIF-1 inhibition by YC-1, 2ME2 and HIF-1 $\alpha$  specific siRNA significantly reduced the protein level of VEGF. These results indicate that high glucose-induced VEGF expression in b.End3 cells depended on HIF-1 activation. To confirm the role of VEGF in high glucose-induced permeability, a VEGF antibody was used to block its effect, as reported previously [21]. As shown in Fig. 7c, d, inhibiting VEGF improved ZO-1 and occludin expression and arrangement and lowered paracellular permeability after high glucose exposure for

6 days. Accordingly, these results support that a plausible pathway for the observed HIF-1-induced permeability in the cells exposed to high glucose may be through VEGF expression.

#### HIF-1 induces permeability increase of human primary brain endothelial cells

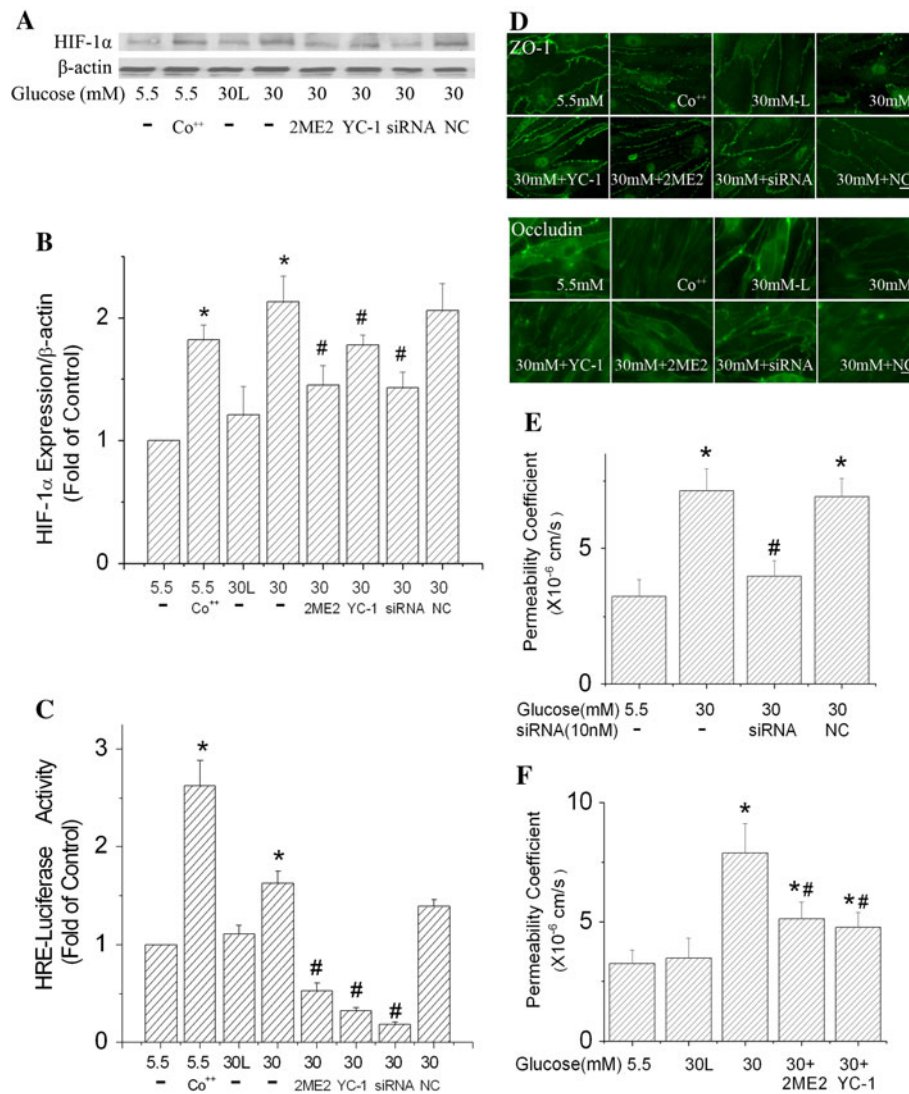
To verify that our results from mouse brain endothelial cells are a real phenomenon, we extended our study to human brain microvascular endothelial cells (hBMVECs). The basal permeability coefficients of hBMVECs to dextran 40 and 70 kDa were  $2.67 \pm 0.42$  and  $0.53 \pm 0.04 \times 10^{-6}$  cm/s, respectively. High glucose increased permeability to both dextran 40 and 70 kDa in hBMVECs (Fig. 8a, b). The effect was time- and concentration-dependent. Similar to our observation in b.End3 cells, changes in the permeability coefficient to dextran 70 kDa were much slower than to dextran 40 kDa. Increasing HIF-1 activity by cobalt chloride significantly elevated the monolayer permeability of hBMVECs after exposed to 5.5 mM glucose for 3, 6 and 10 days. Moreover, the HIF-1 inhibitors, YC-1 and 2ME2, suppressed the increase in permeability induced by 30 mM glucose.

Figure 8c shows that protein levels of ZO-1 and occludin were reduced by high glucose exposure for 6 days and restored by HIF-1 inhibitors in hBMVECs. The ZO-1 level was reduced 48 and 72% by 30 and 50 mM glucose in 6 days, respectively (Fig. 8d). The occludin level was decreased 22 and 27% by 30 and 50 mM glucose, respectively (Fig. 8e). The decreases of both ZO-1 and occludin protein expression were ameliorated by YC-1 and 2ME2. High glucose had no effect on the protein level of claudin-5 in hBMVECs (Fig. 8f).

## Discussion

The study demonstrates that high glucose can induce HIF-1 expression in brain endothelial cells and, for the first time, that HIF-1 contributes to the increase in endothelial permeability caused by high glucose. The present results reveal a new mechanism for high glucose-induced dysfunction of brain endothelia.

Previous studies using animal models have shown that diabetes induces upregulation of HIF-1 $\alpha$  expression in isolated rat hearts [22], rat peripheral nerves [42], mouse kidney mesangial cells [23] and mouse glomeruli [43]. Studies based on samples from diabetic patients have reported increased HIF-1 $\alpha$  expression in human preretinal membranes [44, 45] and mesangial cells [23]. The present report is the first to reveal that high glucose activates HIF-1 $\alpha$  expression in brain vascular endothelial cells. The mechanism of high glucose-induced HIF-1 $\alpha$  expression in



**Fig. 5** Effects of HIF-1 $\alpha$  inhibition on the paracellular permeability of b.End3 cells exposed to high glucose. **a** HIF-1 $\alpha$ -specific siRNA (siRNA) and negative control siRNA (NC) transfection was conducted every 2 days. HIF-1 $\alpha$  inhibitors (10  $\mu$ M YC-1, or 10  $\mu$ M 2ME2) were added to the culture medium 2 h before the onset of high glucose (30 mM) treatments and were added with each medium change (every 2 days). For Co<sup>++</sup> experiments, 100  $\mu$ M CoCl<sub>2</sub> was added to culture medium (5.5 mM glucose) 24 h before the assays. Cells treated with 30 mM L-glucose (30 L) in the presence of 5.5 mM D-glucose served as an osmotic control. **a** Representative Western blots of HIF-1 $\alpha$  with  $\beta$ -actin as a protein-loading control. **b** HIF-1 $\alpha$

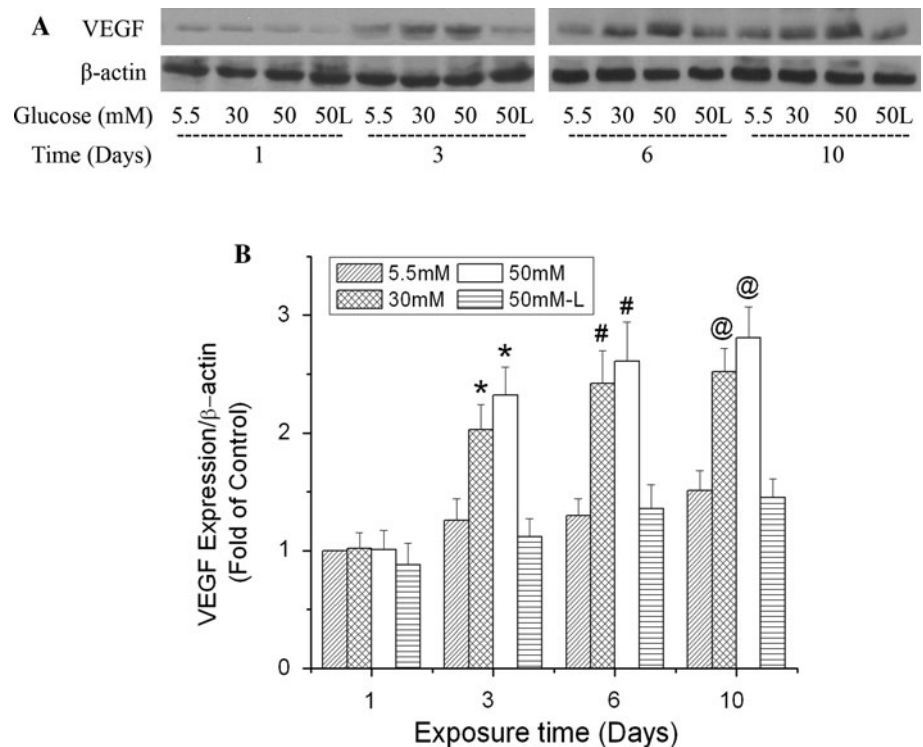
protein expression summarized from three independent experiments. **c** Inhibiting HIF-1 $\alpha$  reduced the increase of HRE-luciferase activity in b.End3 cells. **d** Inhibiting HIF-1 $\alpha$  improved the local distribution of ZO-1 and occludin. *Scale bar* 22  $\mu$ m. **e** Suppression of HIF-1 $\alpha$  expression by siRNA reduced the effect of high glucose on b.End3 paracellular permeability. **f** HIF-1 $\alpha$  inhibitors, 2ME2 and YC-1, ameliorated the increased paracellular permeability caused by 30 mM glucose. Values in **b** and **c** were normalized to  $\beta$ -actin and control (5.5 mM glucose). Values are means  $\pm$  SEM,  $n = 3$ . \* $p < 0.05$  versus control (5.5 mM glucose). # $p < 0.05$  versus 30 mM glucose

brain endothelial cells is not clear. It is well established that HIF-1 $\alpha$  protein is rapidly degraded under normoxia and that the degradation pathway includes HIF-1 $\alpha$  hydroxylation by prolyl hydroxylases (PHDs), binding with von Hippel-Lindau tumor suppressor and degradation by the ubiquitin-proteasome pathway [46]. Under hypoxic conditions, the HIF-1 $\alpha$  level increases because of decreased PHD activities. Besides hypoxia, other factors are capable of

influencing HIF-1 $\alpha$  expression and function under normoxic conditions. Some of these factors are involved in diabetes pathogeny, e.g., advanced glycosylation end products [47] and reactive oxygen species (ROS). In fact, ROS has been reported to stabilize HIF-1 $\alpha$  in cancer cells by inhibiting the activity of PHDs [41, 48], although opposing results have also been observed [49]. Moreover, it has been well reported that high glucose increases ROS



**Fig. 6** Time-dependent effects of high glucose on VEGF expression in b.End3 cells. Cells were treated with glucose at 5.5, 30, and 50 mM for 1, 3, 6 or 10 days. L-Glucose at 50 mM in the presence of 5.5 mM D-glucose was used as osmotic control (50 L). **a** Representative Western blots of VEGF with  $\beta$ -actin as a protein loading control. **b** Summary of three independent experiments. Values were normalized to  $\beta$ -actin and control (5.5 mM glucose, 1 day). Data are means  $\pm$  SEM,  $n = 3$ . \* $p < 0.05$  versus 3 day control (5.5 mM glucose). # $p < 0.05$  versus 6 day control (5.5 mM glucose). @ $p < 0.05$  versus 10 day control (5.5 mM glucose)



production [50–52]. Future investigation is needed to elucidate the molecular mechanism responsible for the activation of HIF-1 in brain endothelial cells.

Another important finding of this study is that HIF-1 contributes to high glucose-induced permeability of brain endothelial cells. The results showed that (1) there was a positive correlation between HIF-1 $\alpha$  expression and endothelial permeability; (2) activating HIF-1 in endothelial cells cultured at normal condition (5.5 mM glucose) induced an increase in permeability; and (3) suppressing HIF-1 activity reduced the permeability increase caused by high glucose. To further confirm the role of HIF-1 and understand the mechanism of HIF-1 in high glucose-induced permeability increase, VEGF expression was examined in the brain endothelial cells exposed to high glucose. As shown in Fig. 6, VEGF expression was elevated time-dependently in high glucose-treated cells. This agrees with previous findings in retinal microvascular endothelial cells [53, 54]. More importantly, HIF-1 inhibition byYC-1, 2ME2 and HIF-1 $\alpha$  siRNA suppressed the VEGF expression induced by high glucose. The results verify that HIF-1 played a role in VEGF expression in the endothelial cells. Nonetheless, we can not conclude that HIF-1 is the sole inducer of the VEGF expression. Other factors may also be responsible for the VEGF expression, such as protein kinase C [55] and peroxisome proliferator-activated receptor  $\gamma$  cofactor-1 $\alpha$  [56].

The brain endothelial tight junction (TJ) consists of the transmembrane proteins such as junctional adhesion

molecule (JAM), occludin, claudin, and accessory proteins, ZO-1 and -2. BBB normally has low permeability due to the presence of TJs [57, 58]. Any alterations of the proteins in expression and arrangement may result in increased permeability. In this study, we examined the expression and arrangement patterns of ZO-1, occludin and claudin-5. High glucose decreased the protein expression of ZO-1 and occludin in a concentration- and time-dependent manner, whereas it had no effect on the claudin-5 protein level. These results coincide with previous reports indicating that diabetes may induce BBB leakage because of arrangement alterations and decreased expression of occludin and ZO-1 but not claudin-5 [9]. The degree of downregulation shown for the ZO-1 and occludin proteins (Fig. 3) seems to be able to induce higher paracellular permeability than that observed. This may be due to stable expression and distribution of claudin-5, which contributes to the lower than expected increase in permeability. The stably expressed claudin-5 may maintain part of the restriction of the tight junction and prevent greater paracellular permeability.

Results from several groups have proven that VEGF is a potent factor in causing endothelial permeability increase [59–61]. It is well studied that VEGF could alter expression and arrangement of TJ proteins, such as ZO-1 and occludin, and increases BBB permeability [9, 15, 21, 62]. Normally, endothelial cells secrete VEGF to the intercellular space, which regulates the intracellular signal pathways through binding to its specific receptor [63].

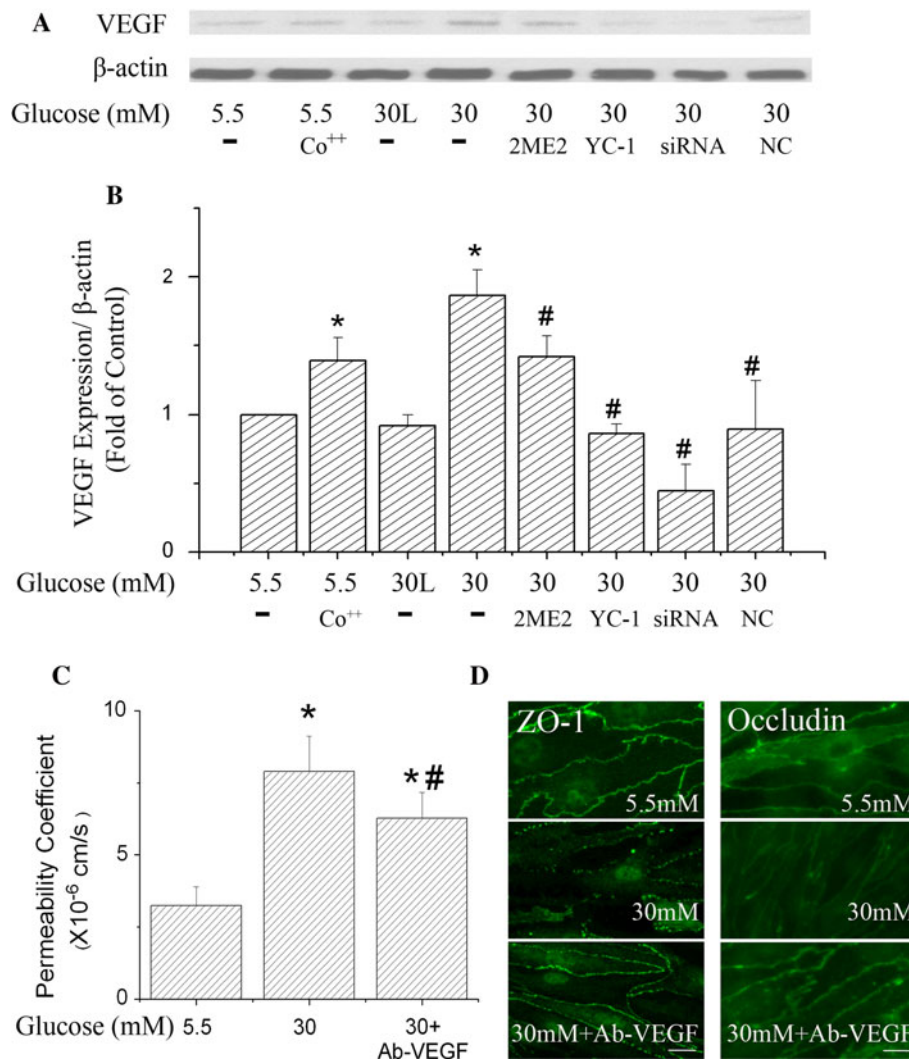


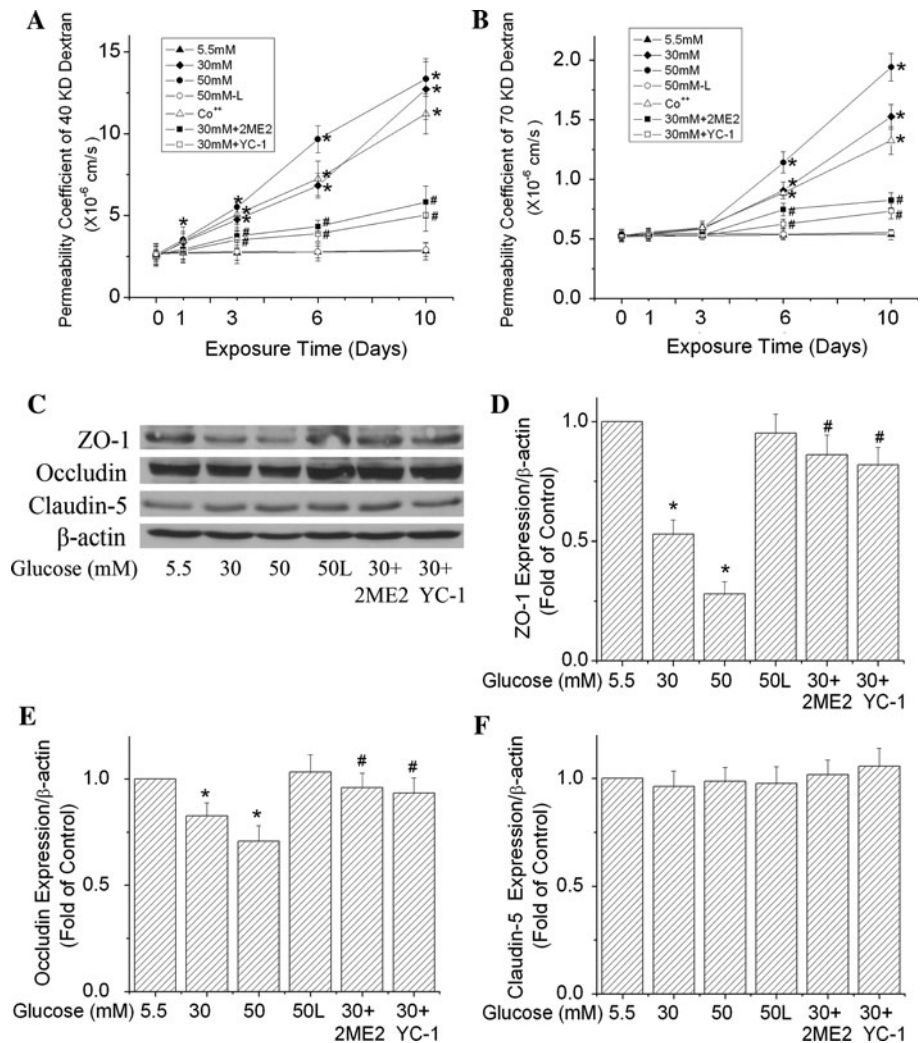
**Fig. 7** Effects of VEGF on the paracellular permeability of b.End3 cells. Cells were treated with 100  $\mu$ M CoCl<sub>2</sub>, HIF-1 $\alpha$  inhibitors (YC-1, 2ME2), HIF-1 $\alpha$ -specific siRNA (siRNA) and negative control siRNA (NC) under the same conditions as described in Fig. 6. VEGF antibody (Ab-VEGF) at 100 ng/ml (final concentration) was added to the cell culture medium 2 h before the high glucose (30 mM) treatment. Cells were incubated in high glucose medium with or without Ab-VEGF for 6 days. The cell culture medium was changed every 2 days with addition of the inhibitors or VEGF antibody to the new culture medium. Cells treated with 30 mM L-glucose (30 L) in

the presence of 5.5 mM D-glucose were used as an osmotic control. **a** Representative Western blots of VEGF expression in b.End3 cells with  $\beta$ -actin as a protein loading control. **b** Summary of VEGF protein expressions from three independent experiments. Values were normalized to  $\beta$ -actin and control (5.5 mM glucose). **c** Effect of Ab-VEGF on permeability of cells exposed to 30 mM high glucose treatment for 6 days. **d** Immunostaining ZO-1 and occludin in b.End3 cells exposed to 30 mM glucose for 6 days. Scale bar 22  $\mu$ m. Data are means  $\pm$  SEM,  $n = 3$ . \* $p < 0.05$  versus control (5.5 mM glucose), # $p < 0.05$  versus 30 mM glucose

VEGF antibodies combine with VEGF protein and block the interaction between VEGF and its receptor. Neutralization of VEGF with its antibodies has been proven to suppress its functions [19, 64]. Our results showed that an VEGF antibody efficiently reduced the increased permeability in cells exposed to high glucose. In addition, the immunostaining images of ZO-1 and occludin revealed that diminished expression and disrupted staining continuity of ZO-1 and occludin were improved by the VEGF antibody. This proves the involvement of VEGF in high glucose-induced paracellular permeability. However, the exact

mechanisms for VEGF-induced TJ protein loss and rearrangement are not completely understood. Two factors might be involved, decrease in mRNA expression and protein phosphorylation. VEGF is able to reduce the mRNA level of ZO-1 [20] and occludin [65]. Furthermore, VEGF may regulate endothelial permeability through phosphorylation of the TJ proteins such as ZO-1 and occludin [59], which are phosphoproteins. Changes in phosphorylation state affect their interaction, alter transmembrane protein localization and induce their redistribution (see review [66] for more details).

**Fig. 8** Effects of high glucose on paracellular permeability and tight junction protein expression of human primary brain microvascular endothelial cells (hBMVECs). hBMVECs were treated with glucose at 5.5, 30 and 50 mM for 1, 3, 6 or 10 days. L-Glucose at 50 mM in the presence of 5.5 mM D-glucose was used as osmotic control. HIF-1 $\alpha$  inhibitors (10  $\mu$ M YC-1, or 10  $\mu$ M 2ME2) were added to the culture medium 2 h before the addition of high glucose (30 mM). In Co<sup>++</sup> experiments, cells were cultured with 5.5 mM glucose in the presence of 100  $\mu$ M cobalt chloride for 1, 3, 6 or 10 days. Paracellular permeability was detected with 40 kDa (a) and 70 kDa (b) FITC-dextran. Permeability was calculated as the absolute values of coefficients. c Representative Western blots of ZO-1, occludin and claudin-5 after cells were exposed to high glucose for 6 days.  $\beta$ -actin served as a protein loading control. Summary of three independent blots of ZO-1 (d), occluding (e) and claudin-5 (f) were illuminated. Values are means  $\pm$  SEM,  $n = 3$ . \* $p < 0.05$  versus control (5.5 mM glucose), # $p < 0.05$  versus 30 mM glucose



The results also demonstrate that the permeability of the b.End3 monolayer is different from that of primary human brain microvessel endothelial cells (hBMVECs). A higher permeability coefficient was observed in b.End3 than in hBMVEC using both 40- and 70-kDa molecular weight tracers. These results indicate that the primary human endothelial cells have a tighter barrier than the mouse cell line. More importantly, the experiments with hBMVECs confirmed our results from b.End3 cells. Similar to the results in b.End3, high glucose increased paracellular permeability and reduced protein levels of ZO-1 and occludin in hBMVECs. HIF-1 inhibitors were also able to restore ZO-1 and occludin levels and ameliorate the increased permeability in the human endothelial cells.

The BBB is formed of several cell types, such as endothelial cells, astrocytes, perivascular microglia, pericytes and neurons, and their interactions determine the BBB function. The results presented in the report are based on an in vitro model of BBB consisting of endothelial cells and have its limitations. However, it provides proof of

principle evidence for future studies with animal models. Our initial results from collaborations with Dr. Rick Dobrowsky have shown that the HIF-1 $\alpha$  protein level is increased in brain microvessels from streptozotocin-treated mice (unpublished data).

In summary, our data have shown that high glucose activates HIF-1 in brain microvascular endothelial cells and that high glucose-induced brain endothelial leakage is mediated by HIF-1-regulated VEGF expression, which is involved in altering the expression and arrangement of tight junction-associated proteins, such as occludin and ZO-1. The results provide a new means for understanding the damaging role of hyperglycemia in brain vasculatures.

**Acknowledgments** We thank Dr. Giovanni Melillo (National Cancer Institute-Frederick, Frederick, MD) for kindly providing us with the PGL2TkHRE plasmid and Dr. Rick Dobrowsky for his valuable suggestions and comments. We are indebted to Drs. Eli Michaelis and Mary Lou Michaelis for reading this manuscript and providing very useful suggestions. This research was supported in part by a KUCR startup fund and a KU NFGF award.

## References

1. Sima AA (2004) Diabetes underlies common neurological disorders. *Ann Neurol* 56(4):459–461. doi:10.1002/ana.20249
2. Ristow M (2004) Neurodegenerative disorders associated with diabetes mellitus. *J Mol Med* 82(8):510–529. doi:10.1007/s00109-004-0552-1
3. The Diabetes Control and Complications Trial Research Group (1993) The effect of intensive treatment of diabetes on the development and progression of long-term complications in insulin-dependent diabetes mellitus. *N Engl J Med* 329(14):977–986. doi:10.1056/NEJM199309303291401
4. UK Prospective Diabetes Study (UKPDS) Group (1998) Intensive blood-glucose control with sulphonylureas or insulin compared with conventional treatment and risk of complications in patients with type 2 diabetes (UKPDS 33). *Lancet* 352(9131):837–853. doi:S0140673698070196
5. Cerbone AM, Macarone-Palmieri N, Saldalamacchia G, Coppola A, Di Minno G, Rivellese AA (2009) Diabetes, vascular complications and antiplatelet therapy: open problems. *Acta Diabetol* 46(4):253–261. doi:10.1007/s00592-008-0079-y
6. Lorenzi M, Healy DP, Hawkins R, Printz JM, Printz MP (1986) Studies on the permeability of the blood–brain barrier in experimental diabetes. *Diabetologia* 29(1):58–62
7. Stauber WT, Ong SH, McCuskey RS (1981) Selective extravascular escape of albumin into the cerebral cortex of the diabetic rat. *Diabetes* 30(6):500–503
8. Huber JD, VanGilder RL, Houser KA (2006) Streptozotocin-induced diabetes progressively increases blood–brain barrier permeability in specific brain regions in rats. *Am J Physiol Heart Circ Physiol* 291(6):H2660–H2668. doi:10.1152/ajpheart.00489.2006
9. Hawkins BT, Lundeen TF, Norwood KM, Brooks HL, Egleton RD (2007) Increased blood–brain barrier permeability and altered tight junctions in experimental diabetes in the rat: contribution of hyperglycaemia and matrix metalloproteinases. *Diabetologia* 50(1):202–211. doi:10.1007/s00125-006-0485-z
10. Mooradian AD, Haas MJ, Batejko O, Hovsepian M, Feman SS (2005) Statins ameliorate endothelial barrier permeability changes in the cerebral tissue of streptozotocin-induced diabetic rats. *Diabetes* 54(10):2977–2982
11. Shivers RR (1979) The effect of hyperglycemia on brain capillary permeability in the lizard, *Anolis carolinensis*. A freeze-fracture analysis of blood–brain barrier pathology. *Brain Res* 170(3):509–522. doi:0006-8993(79)90968-5
12. Iwata A, Koike F, Arasaki K, Tamaki M (1999) Blood brain barrier destruction in hyperglycemic chorea in a patient with poorly controlled diabetes. *J Neurol Sci* 163(1):90–93. doi:S0022510X98003256
13. Starr JM, Wardlaw J, Ferguson K, MacLulich A, Deary IJ, Marshall I (2003) Increased blood–brain barrier permeability in type II diabetes demonstrated by gadolinium magnetic resonance imaging. *J Neurol Neurosurg Psychiatry* 74(1):70–76
14. Bazzoni G, Dejana E (2004) Endothelial cell-to-cell junctions: molecular organization and role in vascular homeostasis. *Physiol Rev* 84(3):869–901. doi:10.1152/physrev.00035.200384/3/869
15. Fischer S, Wobben M, Marti HH, Renz D, Schaper W (2002) Hypoxia-induced hyperpermeability in brain microvessel endothelial cells involves VEGF-mediated changes in the expression of zonula occludens-1. *Microvasc Res* 63(1):70–80. doi:10.1006/mvre.2001.2367
16. Bamforth SD, Kniesel U, Wolburg H, Engelhardt B, Risau W (1999) A dominant mutant of occludin disrupts tight junction structure and function. *J Cell Sci* 112(Pt 12):1879–1888
17. Zlokovic BV (2008) The blood–brain barrier in health and chronic neurodegenerative disorders. *Neuron* 57(2):178–201. doi:10.1016/j.neuron.2008.01.003
18. Forsythe JA, Jiang BH, Iyer NV, Agani F, Leung SW, Koos RD, Semenza GL (1996) Activation of vascular endothelial growth factor gene transcription by hypoxia-inducible factor 1. *Mol Cell Biol* 16(9):4604–4613
19. Schoch HJ, Fischer S, Marti HH (2002) Hypoxia-induced vascular endothelial growth factor expression causes vascular leakage in the brain. *Brain* 125(Pt 11):2549–2557
20. Yeh WL, Lu DY, Lin CJ, Liou HC, Fu WM (2007) Inhibition of hypoxia-induced increase of blood–brain barrier permeability by YC-1 through the antagonism of HIF-1 $\alpha$  accumulation and VEGF expression. *Mol Pharmacol* 72(2):440–449. doi:10.1124/mol.107.036418
21. Bauer AT, Burgers HF, Rabie T, Marti HH (2010) Matrix metalloproteinase-9 mediates hypoxia-induced vascular leakage in the brain via tight junction rearrangement. *J Cereb Blood Flow Metab* 30(4):837–848. doi:10.1038/jcbfm.2009.248
22. Marfella R, D’Amico M, Di Filippo C, Piegari E, Nappo F, Esposito K, Berrino L, Rossi F, Giugliano D (2002) Myocardial infarction in diabetic rats: role of hyperglycaemia on infarct size and early expression of hypoxia-inducible factor 1. *Diabetologia* 45(8):1172–1181. doi:10.1007/s00125-002-0882-x
23. Isoe T, Makino Y, Mizumoto K, Sakagami H, Fujita Y, Honjo J, Takiyama Y, Itoh H, Haneda M (2010) High glucose activates HIF-1-mediated signal transduction in glomerular mesangial cells through a carbohydrate response element binding protein. *Kidney Int* 78(1):48–59. doi:10.1038/ki.2010.99
24. Omid Y, Campbell L, Barar J, Connell D, Akhtar S, Gumbleton M (2003) Evaluation of the immortalised mouse brain capillary endothelial cell line, b.End3, as an in vitro blood–brain barrier model for drug uptake and transport studies. *Brain Res* 990(1–2):95–112. doi:S0006899303034437
25. Li G, Simon MJ, Cancel LM, Shi ZD, Ji X, Tarbell JM, Morrison B 3rd, Fu BM (2010) Permeability of endothelial and astrocyte cocultures: in vitro blood–brain barrier models for drug delivery studies. *Ann Biomed Eng* 38(8):2499–2511. doi:10.1007/s10439-010-0023-5
26. Brown RC, Morris AP, O’Neil RG (2007) Tight junction protein expression and barrier properties of immortalized mouse brain microvessel endothelial cells. *Brain Res* 1130(1):17–30. doi:10.1016/j.brainres.2006.10.083
27. Scott GS, Bowman SR, Smith T, Flower RJ, Bolton C (2007) Glutamate-stimulated peroxynitrite production in a brain-derived endothelial cell line is dependent on *N*-methyl-D-aspartate (NMDA) receptor activation. *Biochem Pharmacol* 73(2):228–236. doi:10.1016/j.bcp.2006.09.021
28. Chen F, Ohashi N, Li W, Eckman C, Nguyen JH (2009) Disruptions of occludin and claudin-5 in brain endothelial cells in vitro and in brains of mice with acute liver failure. *Hepatology* 50(6):1914–1923. doi:10.1002/hep.23203
29. Jacob A, Hack B, Chiang E, Garcia JG, Quigg RJ, Alexander JJ (2010) C5a alters blood–brain barrier integrity in experimental lupus. *FASEB J* 24(6):1682–1688. doi:10.1096/fj.09-138834
30. Betzen C, White R, Zehendner CM, Pietrowski E, Bender B, Luhmann HJ, Kuhlmann CR (2009) Oxidative stress upregulates the NMDA receptor on cerebrovascular endothelium. *Free Radic Biol Med* 47(8):1212–1220. doi:10.1016/j.freeradbiomed.2009.07.034
31. Bernas MJ, Cardoso FL, Daley SK, Weinand ME, Campos AR, Ferreira AJ, Hoying JB, Witte MH, Brites D, Persidsky Y, Ramirez SH, Brito MA (2010) Establishment of primary cultures of human brain microvascular endothelial cells to provide an in vitro cellular model of the blood–brain barrier. *Nat Protoc* 5(7):1265–1272. doi:10.1038/nprot.2010.76



32. Tan W, Rouen S, Barkus KM, Dremina YS, Hui D, Christianson JA, Wright DE, Yoon SO, Dobrowsky RT (2003) Nerve growth factor blocks the glucose-induced down-regulation of caveolin-1 expression in Schwann cells via p75 neurotrophin receptor signaling. *J Biol Chem* 278(25):23151–23162. doi:[10.1074/jbc.M2129](https://doi.org/10.1074/jbc.M2129)
33. Mabejess NJ, Escuin D, LaVallee TM, Pribluda VS, Swartz GM, Johnson MS, Willard MT, Zhong H, Simons JW, Giannakakou P (2003) 2ME2 inhibits tumor growth and angiogenesis by disrupting microtubules and dysregulating HIF. *Cancer Cell* 3(4):363–375
34. Sun HL, Liu YN, Huang YT, Pan SL, Huang DY, Guh JH, Lee FY, Kuo SC, Teng CM (2007) YC-1 inhibits HIF-1 expression in prostate cancer cells: contribution of Akt/NF-kappaB signaling to HIF-1alpha accumulation during hypoxia. *Oncogene* 26(27):3941–3951. doi:[10.1038/sj.onc.1210169](https://doi.org/10.1038/sj.onc.1210169)
35. Ambati J, Canakis CS, Miller JW, Gragoudas ES, Edwards A, Weissgold DJ, Kim I, Delori FC, Adamis AP (2000) Diffusion of high molecular weight compounds through sclera. *Invest Ophthalmol Vis Sci* 41(5):1181–1185
36. Rapisarda A, Uranchimeg B, Scudiero DA, Selby M, Sausville EA, Shoemaker RH, Melillo G (2002) Identification of small molecule inhibitors of hypoxia-inducible factor 1 transcriptional activation pathway. *Cancer Res* 62(15):4316–4324
37. Mikami Y, Hisatsune A, Tashiro T, Isohama Y, Katsuki H (2009) Hypoxia enhances MUC1 expression in a lung adenocarcinoma cell line. *Biochem Biophys Res Commun* 379(4):1060–1065. doi:[10.1016/j.bbrc.2009.01.002](https://doi.org/10.1016/j.bbrc.2009.01.002)
38. Wang GL, Jiang BH, Rue EA, Semenza GL (1995) Hypoxia-inducible factor 1 is a basic-helix-loop-helix-PAS heterodimer regulated by cellular O<sub>2</sub> tension. *Proc Natl Acad Sci USA* 92(12):5510–5514
39. Salceda S, Caro J (1997) Hypoxia-inducible factor 1alpha protein is rapidly degraded by the ubiquitin-proteasome system under normoxic conditions Its stabilization by hypoxia depends on redox-induced changes. *J Biol Chem* 272(36):22642–22647
40. Li Z, Wang D, Messing EM, Wu G (2005) VHL protein-interacting deubiquitinating enzyme 2 deubiquitinates and stabilizes HIF-1alpha. *EMBO Rep* 6(4):373–378. doi:[10.1038/sj.embor.7400377](https://doi.org/10.1038/sj.embor.7400377)
41. Ke Q, Costa M (2006) Hypoxia-inducible factor-1 (HIF-1). *Mol Pharmacol* 70(5):1469–1480. doi:[10.1124/mol.106.027029](https://doi.org/10.1124/mol.106.027029)
42. Chavez JC, Almhanna K, Berti-Mattera LN (2005) Transient expression of hypoxia-inducible factor-1 alpha and target genes in peripheral nerves from diabetic rats. *Neurosci Lett* 374(3):179–182. doi:[10.1016/j.neulet.2004.10.050](https://doi.org/10.1016/j.neulet.2004.10.050)
43. Makino H, Miyamoto Y, Sawai K, Mori K, Mukoyama M, Nakao K, Yoshimasa Y, Suga S (2006) Altered gene expression related to glomerulogenesis and podocyte structure in early diabetic nephropathy of db/db mice and its restoration by pioglitazone. *Diabetes* 55(10):2747–2756. doi:[10.2337/db05-1683](https://doi.org/10.2337/db05-1683)
44. Lim JJ, Spee C, Hinton DR (2010) A comparison of hypoxia-inducible factor-alpha in surgically excised neovascular membranes of patients with diabetes compared with idiopathic epiretinal membranes in nondiabetic patients. *Retina* 30(9):1472–1478. doi:[10.1097/IAE.0b013e3181d6df09](https://doi.org/10.1097/IAE.0b013e3181d6df09)
45. Seftel AD, MacLennan GT, Chen ZJ, Liu S, Ferguson K, Deoreo G, Levine F, Hampel N, Ho-Chang C (1999) Loss of TGFbeta, apoptosis, and Bcl-2 in erectile dysfunction and upregulation of p53 and HIF-1alpha in diabetes-associated erectile dysfunction. *Mol Urol* 3(2):103–107
46. Semenza GL (2001) HIF-1, O(2), and the 3 PHDs: how animal cells signal hypoxia to the nucleus. *Cell* 107(1):1–3
47. Treins C, Giorgetti-Peraldi S, Murdaca J, Van Obberghen E (2001) Regulation of vascular endothelial growth factor expression by advanced glycation end products. *J Biol Chem* 276(47):43836–43841. doi:[10.1074/jbc.M106534200](https://doi.org/10.1074/jbc.M106534200)
48. Klimova T, Chandel NS (2008) Mitochondrial complex III regulates hypoxic activation of HIF. *Cell Death Differ* 15(4):660–666. doi:[10.1038/sj.cdd.4402307](https://doi.org/10.1038/sj.cdd.4402307)
49. Huang LE, Arany Z, Livingston DM, Bunn HF (1996) Activation of hypoxia-inducible transcription factor depends primarily upon redox-sensitive stabilization of its alpha subunit. *J Biol Chem* 271(50):32253–32259
50. Nishikawa T, Araki E (2007) Impact of mitochondrial ROS production in the pathogenesis of diabetes mellitus and its complications. *Antioxid Redox Signal* 9(3):343–353. doi:[10.1089/ars.2007.9.ft-19](https://doi.org/10.1089/ars.2007.9.ft-19)
51. Yamagishi S, Inagaki Y, Amano S, Okamoto T, Takeuchi M, Makita Z (2002) Pigment epithelium-derived factor protects cultured retinal pericytes from advanced glycation end product-induced injury through its antioxidative properties. *Biochem Biophys Res Commun* 296(4):877–882
52. Inoguchi T, Li P, Umeda F, Yu HY, Kakimoto M, Imamura M, Aoki T, Etoh T, Hashimoto T, Naruse M, Sano H, Utsumi H, Nawata H (2000) High glucose level and free fatty acid stimulate reactive oxygen species production through protein kinase C-dependent activation of NAD(P)H oxidase in cultured vascular cells. *Diabetes* 49(11):1939–1945
53. Aiello LP, Pierce EA, Foley ED, Takagi H, Chen H, Riddle L, Ferrara N, King GL, Smith LE (1995) Suppression of retinal neovascularization in vivo by inhibition of vascular endothelial growth factor (VEGF) using soluble VEGF-receptor chimeric proteins. *Proc Natl Acad Sci USA* 92(23):10457–10461
54. Adamis AP, Shima DT, Tolentino MJ, Gragoudas ES, Ferrara N, Folkman J, D'Amore PA, Miller JW (1996) Inhibition of vascular endothelial growth factor prevents retinal ischemia-associated iris neovascularization in a nonhuman primate. *Arch Ophthalmol* 114(1):66–71
55. Poulaki V, Qin W, Jousen AM, Hurlbut P, Wiegand SJ, Rudge J, Yancopoulos GD, Adamis AP (2002) Acute intensive insulin therapy exacerbates diabetic blood-retinal barrier breakdown via hypoxia-inducible factor-1alpha and VEGF. *J Clin Invest* 109(6):805–815. doi:[10.1172/JCI13776](https://doi.org/10.1172/JCI13776)
56. O'Hagan KA, Cocchiglia S, Zhdanov AV, Tambuwala MM, Cummins EP, Monfared M, Agbor TA, Garvey JF, Papkovsky DB, Taylor CT, Allan BB (2009) PGC-1alpha is coupled to HIF-1alpha-dependent gene expression by increasing mitochondrial oxygen consumption in skeletal muscle cells. *Proc Natl Acad Sci U S A* 106(7):2188–2193. doi:[10.1073/pnas.0808801106](https://doi.org/10.1073/pnas.0808801106)
57. Abbott NJ, Patabendige AA, Dolman DE, Yusof SR, Begley DJ (2010) Structure and function of the blood–brain barrier. *Neurobiol Dis* 37(1):13–25. doi:[10.1016/j.nbd.2009.07.030](https://doi.org/10.1016/j.nbd.2009.07.030)
58. Hawkins BT, Davis TP (2005) The blood–brain barrier/neurovascular unit in health and disease. *Pharmacol Rev* 57(2):173–185. doi:[10.1124/pr.57.2.4](https://doi.org/10.1124/pr.57.2.4)
59. Antonetti DA, Barber AJ, Hollinger LA, Wolpert EB, Gardner TW (1999) Vascular endothelial growth factor induces rapid phosphorylation of tight junction proteins occludin and zonula occluden 1 A potential mechanism for vascular permeability in diabetic retinopathy and tumors. *J Biol Chem* 274(33):23463–23467
60. Carpenter TC, Schomberg S, Stenmark KR (2005) Endothelin-mediated increases in lung VEGF content promote vascular leak in young rats exposed to viral infection and hypoxia. *Am J Physiol Lung Cell Mol Physiol* 289(6):L1075–L1082. doi:[10.1152/ajplung.00251.2005](https://doi.org/10.1152/ajplung.00251.2005)
61. Fischer S, Clauss M, Wiesnet M, Renz D, Schaper W, Karliczek GF (1999) Hypoxia induces permeability in brain microvessel endothelial cells via VEGF and NO. *Am J Physiol* 276(4 Pt 1):C812–C820

62. Zhang Z, Chopp M (2002) Vascular endothelial growth factor and angiopoietins in focal cerebral ischemia. *Trends Cardiovasc Med* 12(2):62–66
63. Gitay-Goren H, Cohen T, Tessler S, Soker S, Gengrinovitch S, Rockwell P, Klagsbrun M, Levi BZ, Neufeld G (1996) Selective binding of VEGF121 to one of the three vascular endothelial growth factor receptors of vascular endothelial cells. *J Biol Chem* 271(10):5519–5523
64. Kim KJ, Li B, Winer J, Armanini M, Gillett N, Phillips HS, Ferrara N (1993) Inhibition of vascular endothelial growth factor-induced angiogenesis suppresses tumour growth in vivo. *Nature* 362(6423):841–844. doi:[10.1038/362841a0](https://doi.org/10.1038/362841a0)
65. Argaw AT, Gurfein BT, Zhang Y, Zameer A, John GR (2009) VEGF-mediated disruption of endothelial CLN-5 promotes blood–brain barrier breakdown. *Proc Natl Acad Sci USA* 106(6):1977–1982. doi:[10.1073/pnas.0808698106](https://doi.org/10.1073/pnas.0808698106)
66. Stamatovic SM, Keep RF, Andjelkovic AV (2008) Brain endothelial cell-cell junctions: how to “open” the blood brain barrier. *Curr Neuropharmacol* 6(3):179–192. doi:[10.2174/157015908785777210](https://doi.org/10.2174/157015908785777210)